

## Experimental features of the antiferromagnetism in $\text{Ba}_2\text{GdCu}_3\text{O}_{7-y}$

Zhao Guo-meng,\* Wang Rui-lan, Li Hong-cheng, Qi-ze Ran, Chuan-xing Zhu, Li Lin, and Guan Wei-yan

*Institute of Physics, Chinese Academy of Sciences, Beijing, China*

(Received 21 March 1988; revised manuscript received 24 May 1988)

Structure, resistivity, Meissner effect, magnetization, and specific-heat measurements were conducted on  $\text{Ba}_2\text{GdCu}_3\text{O}_{7-y}$  with different oxygen contents. The results indicate that the local symmetry breaking due to twinning or disorder of oxygen vacancies may give rise to a frustration of the collinear spin structure. The critical behavior of the specific heat is logarithmic but with different amplitudes above and below the transition temperature, implying that the magnetic transition is driven by quasi-three-dimensional magnetic interactions.

The discovery<sup>1</sup> of magnetic ordering at 2.22 K in the high- $T_c$  superconductor  $\text{Ba}_2\text{GdCu}_3\text{O}_{7-y}$  has raised some interesting questions as to the origin of the magnetic ordering, how it affects superconductivity, whether it is two or three dimensional, and whether it is conventional antiferromagnetic (AF) ordering. In this paper, we report resistivity, structure, Meissner effect, magnetization, and specific-heat measurements on  $\text{Ba}_2\text{GdCu}_3\text{O}_{7-y}$  with different oxygen vacancies. The results indicate that oxygen vacancies have no effect on the AF ordering temperature but affect both superconductivity and the magnetic microstructure. The critical behavior of the specific heat is logarithmic but with different amplitudes above and below the ordering temperature, implying the magnetic transition in this system is driven by quasi-three-dimensional (3D) magnetic interactions.

The samples were prepared by mixing powders of  $\text{Gd}_2\text{O}_3$ ,  $\text{CuO}$ , and  $\text{BaCO}_3$  in appropriate ratios. The powders were ground, heated in air at  $930^\circ\text{C}$  for 16 h, and cooled to room temperature within 6 h. Then, the powders were reground, pressed into 13-mm-diameter pellets, sintered at  $970^\circ\text{C}$  for 14 h, and cooled to room temperature within 9 h. Sample 1 was produced by annealing the sintered sample in vacuum ( $\sim 2 \times 10^{-4}$  Torr) at  $800^\circ\text{C}$  for 10 h. Sample 2 was prepared by annealing the

sintered sample in air at  $700^\circ\text{C}$  for 2 h and cooling to room temperature within 3 h. Sample 3 is the sintered sample without further annealing. Sample 4 was obtained by annealing the sintered samples at  $700^\circ\text{C}$  for 15 h and cooling to room temperature within 6 h in flowing oxygen. Samples 5 and 6 were produced by annealing the sintered samples in different tubes at  $800^\circ\text{C}$  for 15 h and cooling to room temperature within 6 h in flowing oxygen.

X-ray diffraction analysis was carried out on a monochromated  $\text{Cu } K\alpha$  radiation. The standard four-probe technique was used to measure the resistivity. The magnetization and Meissner-effect measurements were made on an extracting magnetometer in which the magnetic field could be continuously varied from  $0-8 \times 10^4$  Oe, the inhomogeneity of the field being less than  $10^{-4}$  over a diameter of 60 mm. The temperature was computer controlled within a range of 1.5–300 K with an accuracy of

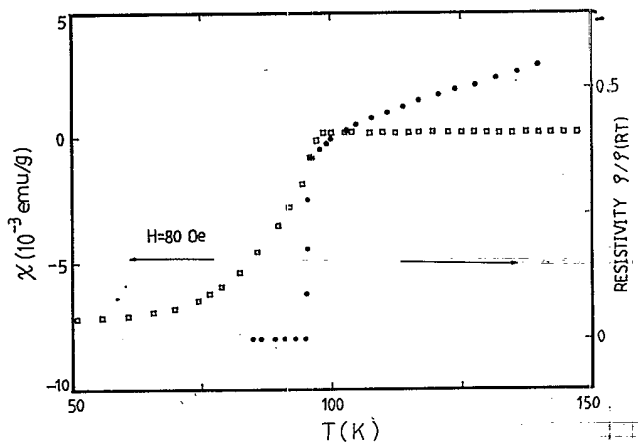


FIG. 1. Temperature dependence of resistivity (●) and susceptibility (□) of sample 4 annealed in flowing oxygen.

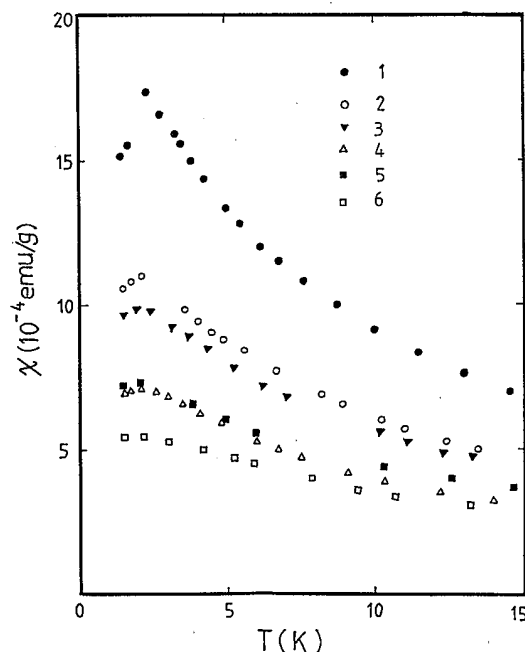


FIG. 2. Susceptibility results for all the six samples cooled in 10 kOe. The number labeled in the figure corresponds to the sample number.

TABLE I. Electrical and magnetic properties of the six samples.

Sample No.	$T_{cl}$ (K)	$\Delta T_c$ (K)	MF (%)	$\Theta$ (K)	$P_{eff}$ ( $\mu_B$ )	$T_p$ (K)	SM (emu/g)	$T_N$ (K)
1	...	...	...	6.0	8.0	2.2	53	2.2
2	...	5.0	35	3.5	8.0	2.2		2.23
3	89.0	3.0	50	4.0	8.0	2.2		
4	95.0	1.0	62	2.0	8.0	2.1	42	
5	94.0	2.0	40	3.0	8.0	2.1		
6	94.5	1.5	43	3.0	8.0	...	36	2.23

$\pm 0.01$  K. The experimental error of the magnetization measurement was better than  $5 \times 10^{-4}$  emu.

The specific heat was measured using the adiabatic method. To make samples heat uniformly and reach thermal equilibrium quickly, we wrapped them in a piece of thin copper foil to which a carbon resistor thermometer and heater were attached. The rate of temperature shift was better than 0.5 mK/min. The background has been subtracted from all the data shown.

The temperature dependence of resistivity for sample 4 is shown in Fig. 1 (solid circle). The sample exhibits a good metallic behavior with  $\rho(300 \text{ K}) \approx 900 \mu\Omega \text{ cm}$  and  $\rho(300)/\rho(100 \text{ K}) \sim 2.5$ , and a transition width of 1.0 K. The Meissner flux expulsion for the sample (open square) reached about 62% at 20 K with no paramagnetism correction. Sample 1 shows a semiconducting behavior and sample 2 shows some superconductivity; however, there is no zero-resistance state down to 4.2 K. The other samples exhibit good superconductivity with orthorhombic structure. Sample 1 has tetragonal structure. The electric and magnetic properties for all six samples are shown in Table I.

Figure 2 shows the susceptibility of the six samples cooled in a field of 10 kOe. As the oxygen content increases, the kinks in these curves are gradually smeared out and the magnitudes of the susceptibility are correspondingly depressed. An amazing result is curve 6 which shows no kink but saturates below 2.2 K. The susceptibility between 1.5 and 300 K for sample 6 cooled in a field of 10 kOe is plotted in Fig. 3. The susceptibility at low temperature is too small and deviates substantially from the Curie-Weiss law which is valid at higher temperatures.

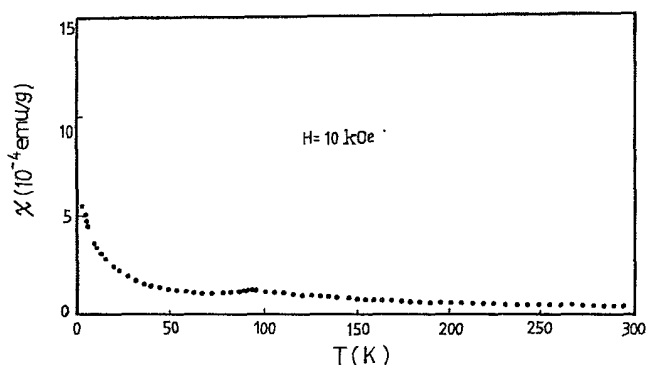


FIG. 3. Susceptibility of sample 6 in the temperature range 1.5–300 K.

The diamagnetic susceptibility in such a high field is too small [ $\sim 1.0 \times 10^{-4}$  emu/g as seen from nonmagnetic superconducting  $\text{Ba}_2\text{YCu}_3\text{O}_{7-y}$  (Ref. 2)] to account for such a large deviation ( $\sim 20 \times 10^{-4}$  emu/g at 1.5 K) even if one considers the screening effect of paramagnetism due to flux expulsion. Thus, the remaining possibility is that the paramagnetic susceptibility itself might deviate from the Curie-Weiss law at lower temperatures. The reduced Curie constant or effective moment at lower temperatures may originate from crystal field effect. However, such an effect is very small as seen from specific-heat experiments.<sup>3</sup> Another possibility is that the spin-spin correlation is so strong above  $T_N$  that the deviation of paramagnetism from the Curie-Weiss law occurs at a temperature well above  $T_N$ . If this is true, one should observe a similar deviation in sample 1. In fact, no deviation has been found in sample 1. Furthermore, it is worth noting that the Curie temperatures for orthorhombic samples are depressed compared with those for tetragonal samples as shown in Table I and Refs. 4 and 5.

The magnetization via field at 1.5 K for samples 1 and 6 are shown in Fig. 4. Both curves saturate at high fields but the saturation magnetizations of the samples are very different even though they have almost the same effective moment at high temperatures. The saturation magnetization of sample 1 (open square) is about 53 emu/g, very close to the ideal value ( $\sim 54$  emu/g), and that of sample

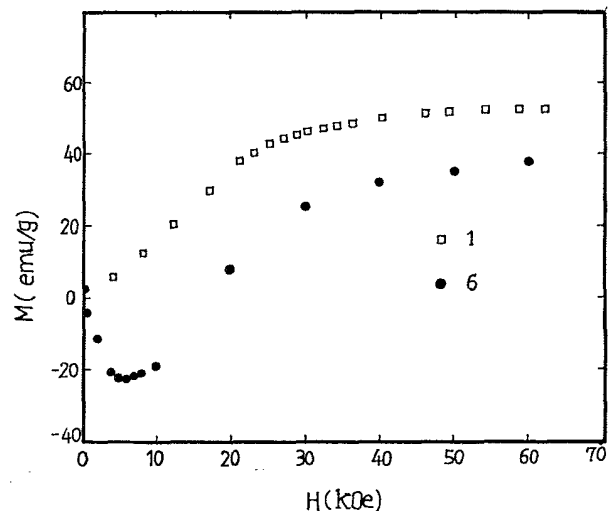


FIG. 4. Magnetization curves at 1.5 K for sample 1 ( $\square$ ) and sample 6 ( $\bullet$ ).

6 (solid circle) is about 36 emu/g, 80% of the ideal value even with diamagnetic correction ( $\sim 4\text{--}8$  emu/g as seen from  $\text{Ba}_2\text{YCu}_3\text{O}_{7-y}$ ). The reduction of the saturation magnetization at 1.5 K was also observed in some nonsuperconducting tetragonal samples ( $\sim 42$  emu/g, Ref. 4) although they have ideal effective moments at higher temperatures. Therefore, the low-temperature moment in this system varies from sample to sample possibly due to the variation of the microstructure of crystal which leads to different local symmetry.

In Fig. 5, we show specific-heat results for samples 2

$$C_m = 2R(2\beta_N\epsilon)^2/\pi[-2\ln(T/T_N - 1) + 2\ln(1/2\beta_N\epsilon) - (1 + \pi/4)], \quad T > T_N \quad (1)$$

and

$$C_m = 2R(2\beta_N\epsilon')^2/\pi[-2\ln(1 - T/T_N) + 2\ln(1/2\beta_N\epsilon') - (1 + \pi/4)] + B, \quad T < T_N, \quad (2)$$

where  $\beta_N = 1/k_B T_N$ ,  $2.269\beta_N\epsilon = 1$ ,  $2.643\beta_N\epsilon' = 1$ ,  $B = 5.4$  J/mol K, and  $T_N = 2.23$  K. The exact solution of the 2D Ising model has the following critical behavior:<sup>6</sup>

$$C_m^I = 2R(2\beta_N\epsilon)^2/\pi[-\ln|1 - T/T_N| + \ln(1/2\beta_N\epsilon) - (1 + \pi/4)]. \quad (3)$$

It has the same amplitude above and below  $T_N$ . Otherwise, the asymmetric amplitudes in the  $\text{Ba}_2\text{GdCu}_3\text{O}_{7-y}$  system lead us to suggest that the magnetic transition should be driven by quasi-3D magnetic interactions even if the distance between Gd planes is fairly large ( $\sim 11.7$  Å). However, we do not believe that the magnetic interaction is purely a 3D dipolar one which would predict a logarithm to the one-third power with different amplitudes above and below  $T_N$ .<sup>7</sup> Therefore, the magnetism of  $\text{Ba}_2\text{GdCu}_3\text{O}_{7-y}$  cannot purely be described by the 2D Ising or 3D dipolar model but possibly by a mixed model of the two.

The low-temperature specific heat, according to spin-wave theory, should follow  $T^2$  and  $T^3$  laws for 2D and 3D collinear antiferromagnetic systems. Any deviation from the collinear spin structure might make the observed behavior deviate from these laws. The complex structure in the low-temperature specific heat<sup>5</sup> leads us to suggest that

and 6 as  $C/T$  vs  $T$ . Both the samples have the same magnetic transition temperature (2.23 K) though they have different electrical and magnetic properties. An interesting result is that the two curves are coincident above  $T_N$  but a little different ( $\sim 5\%$ ) below  $T_N$  (open square for sample 2 and solid triangle for sample 6).

Figure 6 shows the critical behavior of the specific heat for sample 6 as  $C_m$  vs  $\ln|T - T_N|$ . The curves both exhibit a good linearity near  $T_N$  but have different slopes.  $C_m$  can be fitted as

the spin structure at absolute zero in these samples might not be strictly collinear. On the other hand, the slight difference of specific heat below  $T_N$  for samples 2 and 6 might imply that their spin structures may be a little different since the same spin structure and magnetic ordering temperature should correspond to the same thermodynamic behavior. One possibility is that the spin directions of the two are slightly different if they are both collinear antiferromagnets. Another possibility is that they have, to some degree, a noncollinear spin structure which may not be a unique ground state.<sup>8</sup> The noncollinearity could also account for observed magnetic properties such as reduced saturation magnetization at low temperatures even in some nonsuperconducting samples, reduced Curie temperature (0.9 K in Ref. 5), reduced Curie constant at low temperatures for our orthorhombic samples as discussed above, and the smearing of susceptibility

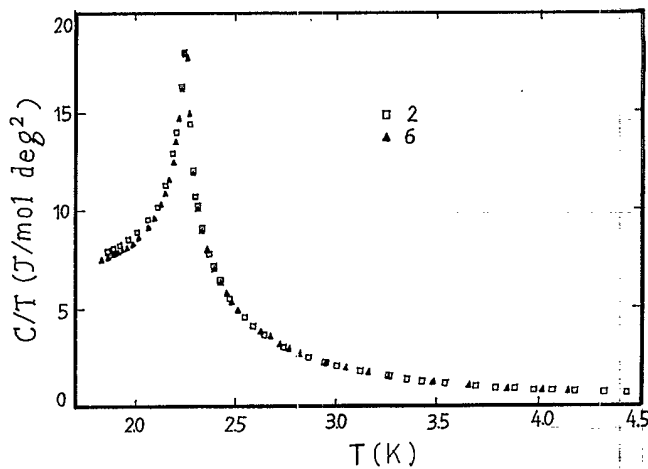


FIG. 5. Low-temperature specific heat for sample 6 ( $\blacktriangle$ ) and sample 2 ( $\square$ ).

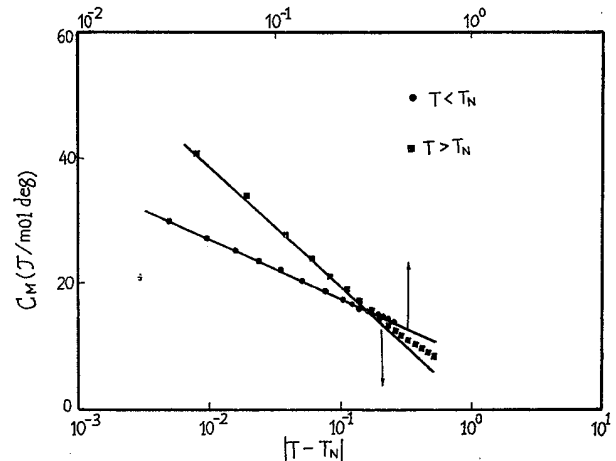


FIG. 6. Critical behavior of specific heat for sample 6. The linear behaviors remain within the larger temperature range ( $> 0.1$  K) near  $T_N$ .

kinks at the ordering temperature. The possible noncollinearity in orthorhombic samples might originate from coherent twin boundaries that are formed at lower temperatures<sup>9</sup> due to a tetragonal-to-orthorhombic transition at higher temperature. The local symmetry breaking due to twinning in orthorhombic samples and possible disordered distribution of oxygen vacancies in some tetragonal samples could give rise to complex magnetic interactions which make it difficult to form a strictly collinear spin structure. Our tetragonal sample must be different from that in Ref. 4 in the crystal microstructures and may be a collinear antiferromagnet.

Oxygen vacancies have great effects on the electrical properties or electronic states at the Fermi level but no effect on  $T_N$ . This implies that conduction electrons decouple from magnetic ions and that the magnetic interaction could not be the Ruderman-Kittel-Kasuya-Yosida interaction. We believe that the in-plane dipolar magnetic interaction should be dominant and interplane coupling might not be strong.

The authors would like to thank Dr. Zhao Yu-ying for x-ray analysis. The project is supported by the National Natural Science Foundation of China.

---

\*On leave at the Department of Physics, University of Southern California, Los Angeles, Los Angeles, CA 90089-0484.

<sup>1</sup>J. C. Ho, P. H. Hor, R. L. Meng, C. W. Chu, and C. Y. Huang, *Solid State Commun.* **63**, 711 (1987).

<sup>2</sup>Chin Lin *et al.*, *Solid State Commun.* **63**, 1129 (1987).

<sup>3</sup>B. W. Lee *et al.*, *Phys. Rev. B* **37**, 2368 (1988).

<sup>4</sup>Chin Lin *et al.*, *Solid State Commun.* **64**, 691 (1987).

<sup>5</sup>B. D. Dunlap *et al.* (unpublished).

<sup>6</sup>L. Onsager, *Phys. Rev.* **65**, 117 (1944).

<sup>7</sup>P. Beauvillain *et al.*, *J. Magn. Magn. Mater.* **15-18**, 421 (1980).

<sup>8</sup>Kishin Moorjani and J. M. D. Coey, *Magnetic Glasses* (Elsevier, Amsterdam, 1984).

<sup>9</sup>F. M. Mueller *et al.*, *Phys. Rev. B* **37**, 5837 (1988).